AIP | Physics of Fluids

On the hydrodynamic interaction between a particle and a permeable surface

Guy Z. Ramon, Herbert E. Huppert, John R. Lister, and Howard A. Stone

Citation: Phys. Fluids **25**, 073103 (2013); doi: 10.1063/1.4812832
View online: http://dx.doi.org/10.1063/1.4812832
View Table of Contents: http://pof.aip.org/resource/1/PHFLE6/v25/i7
Published by the AIP Publishing LLC.

PHYSICS OF FLUIDS **25**, 073103 (2013)

On the hydrodynamic interaction between a particle and a permeable surface

Guy Z. Ramon,[1,a),b)] Herbert E. Huppert,[2,3,4] John R. Lister,[2] and Howard A. Stone[1,a)]
[1]*Department of Mechanical and Aerospace Engineering, Princeton University, Princeton, New Jersey 08544, USA*
[2]*Institute of Theoretical Geophysics, DAMTP, Centre for Mathematical Science, University of Cambridge, Cambridge CB3 OWA, United Kingdom*
[3]*School of Mathematics, University of New South Wales, Kensington 2052, Australia*
[4]*Faculty of Science, Bristol University, Bristol Avon, BS2 8BB, United Kingdom*

(Received 23 January 2013; accepted 6 June 2013; published online 26 July 2013)

The motion and deposition of a particle translating perpendicular to a rigid, permeable surface is considered. The lubrication approximation is used to derive an equation for the pressure in the gap between the particle and the permeable surface, with a symmetric shape prescribed for the particle. The hydrodynamic force on a particle is, in general, a function of the particle size and shape, the distance from the surface and the surface permeability, and its sign depends on the relative motion of the particle and the background fluid permeating through the surface. As the particle becomes flatter, this force generally increases and is more sensitive to the surface permeability. In the case of a spherical particle, closed-form, approximate solutions are obtained using perturbation methods, in the limits of small permeability and close approach to contact. It is also shown that a sedimenting particle attains a finite velocity on close approach, which scales as $k^{1/2}$ and k for a sphere and a disc, respectively, where k is the permeability per unit thickness of the surface. In the case of a particle advected toward the surface, as is common in membrane filtration, a balance of electrostatic repulsion and viscous drag is used to calculate a possible equilibrium position of the particle, at some finite distance from the surface. The dependence of the equilibrium and its stability is shown in terms of the ratio of electrostatic and lubrication forces at contact, as well as the ratio of characteristic lengths over which the two forces decay away from the boundary. The latter is found to be a significant factor in determining the conditions under which a stable equilibrium exists. These results are useful for estimating deposition propensity in membrane filtration processes, as affected by operational conditions. [http://dx.doi.org/10.1063/1.4812832]

I. INTRODUCTION

When a spherical particle slowly approaches a solid, impermeable boundary, consideration of hydrodynamic interactions predicts a force resisting the approach. For a constant particle velocity, this force is inversely proportional to the separation distance. The theory also predicts that, when the particle motion is driven by a constant external force (e.g., gravity), an infinite time is required for actual contact to be made with a smooth, planar boundary (see, for example, Ref. 1). This result is relaxed when the interacting surfaces are rough, the fluid is compressible, or when either or both surfaces are compliant.[2–5] A finite force at contact has also been shown to occur when the solid

[a)]Authors to whom correspondence should be addressed. Electronic addresses: ramong@technion.ac.il and hastone@princeton.edu.
[b)]Also at Department of Civil and Environmental Engineering, Technion-Israel Institute of Technology, Haifa 32000, Israel.

boundary is permeable. This case was first studied by Goren,[6] who solved the Stokes flow problem in bi-spherical coordinates for a sphere approaching a thin permeable layer, for example, a membrane of thickness ℓ_m and permeability k^*. The force at contact scales as $(R/k)^{1/2}$, with R the radius of the sphere and $k = k^*/\ell_m$ the membrane permeability per unit thickness. This result was later confirmed by Nir,[7] who specifically treated the contact problem using tangent-sphere coordinates. In a related problem, Sherwood[8] considered the force required to pull a sphere away from contact with a porous half-space, in which case the force scales as $(R^2/k^*)^{2/5}$ as $k^* \to 0$, while for the case of a flat disc, the force scales as R^2/k^*. The half-space differs from the thin membrane by the effective length over which the fluid must flow through (ℓ_m for the membrane) and the presence of a radial flow component in the porous medium.

Other related studies considered the flow field and forces due to the motion of spherical porous particles, in which the fluid in the porous layer obeys either a Darcy equation with a Beavers-Joseph slip condition for the tangential velocity at the fluid-solid interface[9,10] or a Brinkman equation.[11] More recently, the Green's function for the Stokes flow near a porous slab, derived by Elasmi and Feuillebois,[12] has been extended to consider a sphere adjacent to a thin permeable slab, employing either a boundary integral form[13] or a distribution of singularities.[14] A summary of these representative studies, the general problem treated and methods employed, is presented in Table I, along with the themes of the present study.

The previously described theoretical frameworks all implicitly assume a scale separation between the characteristic sizes of the particle and pores. This assumption is supported, for example, by numerical calculations of the force on a sphere approaching a pore.[15] The results showed that for a sphere of radius R, ten times greater than the pore size, r_p, the force at a separation distance of $0.1R$ deviates by only $\sim$8% from that predicted for the force near an impermeable wall. In fact, with the geometry used by Yan *et al.*,[15] one may approximate the effective permeability of a single cylindrical pore in an area equivalent to the projection of an approaching, co-centric sphere as $k \approx \phi r_p^2$, where r_p is the pore radius and $\phi \approx (r_p/R)^2$ is the effective surface porosity. Based on this approximation, a similar deviation of the force is predicted under an assumption of uniform permeability.[6,16] Comparing these two approaches, it appears that the difference between accounting for the pore dimensions and the uniform permeability assumption is not significant, and generally below 10%. Thus, for

TABLE I. Summary of studies on particle interactions with porous boundaries.

Author	Problem treated	Method	Remarks
Goren[6]	Sphere translating to thin porous layer	Series solution of Stokes equations in bi-spherical coordinates	Semi-analytical series solution
Nir[7]	Sphere in contact with thin porous layer	Stokes equations in tangent-sphere coordinates, reduction to ODE	Asymptotics for high/low permeability
Sherwood[8]	Sphere in contact with semi-infinite porous layer	Stokes equations in tangent-sphere coordinates, reduction to ODE	Asymptotics for high/low permeability
Michalopoulou *et al.*[9,10]	Porous/solid spheres in relative motion, with background flow	Stokes equations in bi-spherical coordinates, slip boundary condition	Semi-analytical series solution
Davis[11]	Porous sphere moving toward solid wall or porous sphere	Stokes equations in bi-spherical coordinates, with Brinkman equations	Semi-analytical series solution
Elasmi and Feuillebois[13]	Flow around sphere near thin porous layer	Stokes equations in boundary integral form	Numerical
Debbech *et al.*[14]	Flow around sphere near thin porous layer	Fundamental solution of Stokes equations	Minimizing functional of singularity distribution
This paper	Symmetric shape in background flow, near thin porous layer	Lubrication approximation	Asymptotics and scaling analysis

$R \gg r_p$ the use of a macroscopically defined permeability is reasonably accurate and will also be made in the forthcoming analysis.

In the case of an object sedimenting under gravity onto a surface, the motion of the particle will be modified by a resistive force, dependent on the permeability of the surface as well as the size and shape of the object. A different configuration may be motivated by filtration processes. The hydrodynamic force on a particle in the vicinity of a permeable wall is important to membrane separation applications, where particle deposition is a major concern, leading to productivity loss and increased energy consumption.[17] A useful way of predicting colloidal deposition in such systems is made through a force balance accounting for surface interactions (e.g., electrostatic repulsion) and the hydrodynamic "permeation drag."[18] The latter is caused by the presence of a background flow, which advects material toward the membrane surface. It has recently been shown that for values representative of practical membrane properties, this force can be orders of magnitude larger than the Stokes drag in an unbounded fluid.[16] Hence, a proper account of the hydrodynamic force is crucial for any quantitative assessment of deposition propensity.

In this paper, we examine the problem of a particle approaching a thin permeable wall. Specifically, we consider the hydrodynamic interaction at a close distance, smaller than the particle radius. A lubrication model is formulated, which is then used to explore the dynamics of the particle approach to the surface and shape effects, with asymptotic forms found for the specific cases of near contact, and a spherical particle. In Sec. II, we formulate the problem and the governing lubrication equations. A perturbation analysis is presented in Sec. III, followed by calculations of the pressure field and resulting force on the particle at close approach, as affected by the particle shape, in Sec. IV. In Sec. V, the dynamics of the particle motion and deposition are presented. Finally, Sec. VI presents our conclusions in brief form.

II. MODEL FORMULATION

We consider a particle immersed in an incompressible flow of a Newtonian fluid with constant dynamic viscosity, μ, in close proximity to a permeable planar surface (see the schematic drawing in Fig. 1(a)). Following Stone,[19] the surface of the particle is modeled as a generalized symmetric shape given by $z = \delta + R - (R^n - r^n)^{1/n}$, where r, z denote the radial and vertical coordinates, respectively, $\delta(t)$ is the distance of closest approach, n is an even integer and R is a characteristic length that would correspond with the radius in the case of a spherical object ($n = 2$, see Fig. 1(b)). For $n > 2$, these shapes have zero local curvature at the point of closest approach. It is further assumed that the planar surface is uniformly permeable. As discussed above, this assumption corresponds to a requirement that there exists a scale separation between the characteristic pore-size, r_p, and particle size; indeed,

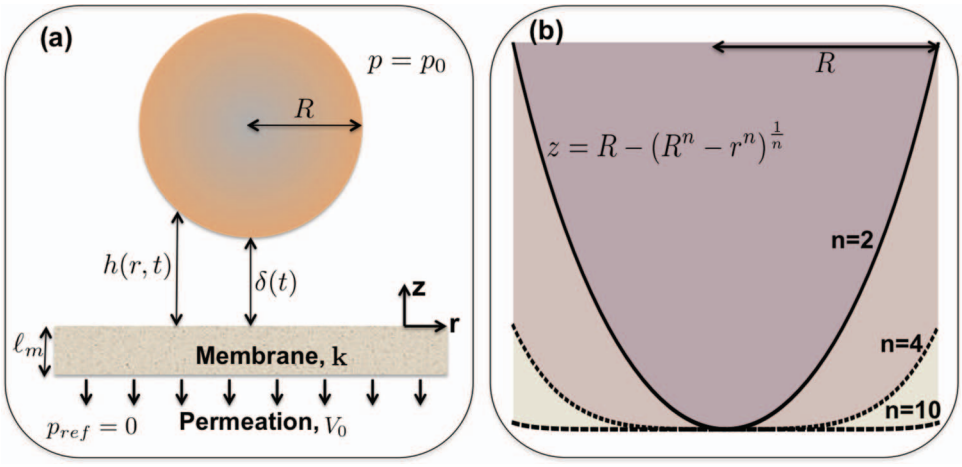

FIG. 1. (a) Schematic illustration of the problem geometry. (b) The generalized, symmetric shape used to model the particle, shown for $n = 2, 4, 10$.

in what follows it will be assumed that $R \gg r_p$. Only translational motion, perpendicular to the surface, will be considered with no rotation of the particle.

The hydrodynamic interaction between the particle and the wall is due to the "squeezing" of liquid in the region confined by the two solid boundaries, which results in additional stresses. In the case of a permeable wall, the liquid may be driven into or out of the gap, depending on the relative motion of the sphere and the background flow. The axisymmetric velocity field (u, w) within this gap is well described by the classical "lubrication approximation" (see, for example, Leal[20] and Oron *et al.*[21]), which is satisfied when $\delta \ll R$. Under this approximation, the equations of motion reduce to

$$\frac{\partial p}{\partial r} = \mu \frac{\partial^2 u}{\partial z^2}, \quad \frac{\partial p}{\partial z} = 0, \tag{1}$$

while the continuity equation is

$$\frac{1}{r}\frac{\partial}{\partial r}(ru) + \frac{\partial w}{\partial z} = 0, \tag{2}$$

in which u, w are the velocity components in the r and z directions, respectively, and p is the pressure.

At the solid surfaces, a no-slip condition holds for the radial velocity, i.e.,

$$u(0) = u(h) = 0, \tag{3}$$

where $h = h(r, t)$ is the gap between the sphere surface and the wall, which may be approximated, using the first term in a Taylor series of the shape described above, as

$$h(r, t) = \delta(t) + \frac{r^n}{nR^{n-1}} + O\left(\frac{r^{2n}}{R^{2n-1}}\right), \tag{4}$$

with $\delta(t)$ denoting the minimum gap distance (see Fig. 1). We do not consider the possibility of slip at the porous surface, consistent with the absence of a radial velocity component within the thin porous membrane.

The boundary conditions on w, the z-component of the velocity, are prescribed through a kinematic relation that accounts for the possible motion of each surface, as well as the fluid flux through the permeable boundary. Thus, at the particle surface

$$w(z = h) = \frac{d\delta}{dt}, \tag{5}$$

where $d\delta/dt \equiv -V_p$ is the velocity of the rigid particle; $V_p > 0$ then corresponds with motion toward the membrane. We further define the background permeation V_0, forced through the membrane by the imposed background pressure p_0, as

$$V_0 \equiv \frac{k^*}{\mu}\left(\frac{p_0 - p_{ref}}{\ell_m}\right), \tag{6}$$

in which p_{ref} is the pressure on the other side of the membrane, k^* is the Darcy permeability and ℓ_m the membrane thickness (in what follows, these two are lumped and we use the permeance $k = k^*/\ell_m$). In the absence of the particle, this uniform flow would be the state of the system. We note that in the case considered here, the pressure drop is driving the flow downward through the membrane, i.e. $p_0 > p_{ref}$, but this may be reversed if the downstream pressure is higher than the background fluid pressure, $p_{ref} > p_0$. In what follows, and without loss of generality, we take p_{ref} to be identically zero.

The downward motion of the sphere relative to the surface will lead to an increase or decrease of the pressure (and, hence, the permeation), depending on the sign of the difference in relative velocities of the particle and background fluid, $V_p - V_0$. For example, if the particle moves faster than the background fluid, as would occur if it is acted upon by an external force directed toward the membrane, the pressure in the gap would increase at the approach of the particle, resulting in a resistive hydrodynamic force. If, on the other hand, the fluid motion is faster than the particle, as

may occur if there is a repulsive interaction between the particle and the surface (e.g., electrostatic), then the pressure in the gap will decrease relative to the background pressure.

Additional permeation is induced by the pressure increase/decrease within the gap. Noting that under the lubrication approximation, the pressure does not vary with z (see Eq. (1)), the fluid flux at the boundary may be related directly to the pressure at any radial location by

$$w(z=0) = -\frac{k^*}{\mu}\frac{dp_m}{dz} = -\frac{k}{\mu}p|_{z=0}, \tag{7}$$

where p_m refers to the pressure in the membrane and, as in (6), $p_{ref} = 0$. The derivation procedure is now straightforward. Integrating (1) twice using (3), substituting into (2) and integrating across the gap, we obtain

$$w(h) - w(0) = \frac{1}{12\mu r}\frac{\partial}{\partial r}\left(rh^3\frac{\partial p}{\partial r}\right), \tag{8}$$

which, upon substitution of the boundary conditions given by (5) and (7), results in

$$\frac{1}{12\mu r}\frac{d}{dr}\left(rh^3\frac{dp}{dr}\right) - \frac{k}{\mu}p + V_p = 0, \tag{9}$$

for the pressure within the gap, where we now use ordinary derivatives since the pressure is regarded as quasi-steady and only implicitly time-dependent through the particle motion. This equation is to be solved subject to the boundary conditions

$$\frac{dp}{dr} = 0 \quad \text{at} \quad r = 0, \tag{10}$$

from symmetry considerations and

$$p = p_0 \quad \text{as} \quad r \to \infty. \tag{11}$$

It is convenient to re-write (9) in terms of the 'excess' pressure in the fluid relative to the background pressure p_0, i.e., $\hat{p} = p - p_0$. Since $kp_0/\mu \equiv V_0$, we have

$$\frac{1}{12\mu r}\frac{d}{dr}\left(rh^3\frac{d\hat{p}}{dr}\right) - \frac{k}{\mu}\hat{p} + (V_p - V_0) = 0, \tag{12}$$

and the excess pressure $\hat{p}$ decays to zero far from the sphere. This equation illustrates that, dependent on the relative motion of the permeating fluid and the particle, the pressure within the gap (relative to the background pressure p_0) can be either positive ($V_p > V_0$) or negative ($V_0 > V_p$).

A. The scaled equation

Equation (12) is made non-dimensional by scaling r with the characteristic gap length-scale,

$$\ell_n = (n\delta R^{n-1})^{1/n}, \tag{13}$$

and h by δ, while the velocity scale is taken as $V \equiv V_p - V_0$, the velocity of the particle relative to the background fluid. Based on these, the pressure scale is chosen as $\hat{p} = (12\mu V\ell_n^2/\delta^3)P$. With these scaling transformations, the resulting equation becomes

$$\frac{1}{s}\frac{d}{ds}\left(sH^3\frac{dP}{ds}\right) - \beta P + 1 = 0, \tag{14}$$

in which $s = r/\ell_n$,

$$\beta = \frac{12k\ell_n^2}{\delta^3} \tag{15}$$

is the permeability parameter and the scaled gap height is now given as $H = 1 + s^n$. The corresponding boundary conditions are

$$P(\infty) = 0, \quad \frac{dP}{ds}|_{s=0} = 0. \tag{16}$$

B. The force on the particle

In the lubrication regime, the z-component of the dimensional force f on the particle may be calculated by integrating the pressure within the gap, and hence we define a scaled force

$$F_n = \frac{f}{24 c_n \pi \mu V \ell_n^4/\delta^3} = c_n^{-1} \int_0^\infty s P(s)\, \mathrm{d}s, \tag{17}$$

where $c_n = \int_0^\infty s P(s;\beta = 0)\, \mathrm{d}s$. Under this choice of scaling, the reference force is that for a squeeze flow with an impermeable wall. For example, in the case of a spherical particle, $c_2 = 1/16$ and the reference force becomes $6\pi\mu V R^2/\delta$ since $\ell_2 = (2R\delta)^{1/2}$. For general n, the numerical constants are, for example, $c_4 = 1/32$ and $c_{10} = 1/25$ and it has been shown by Stone[19] that this reference force scales as $\delta^{4/n-3} R^{4(n-1)/n}$.

III. ASYMPTOTIC ANALYSIS

A. Approach to contact

To establish typical orders of magnitude, it is convenient to work with the dimensional equation (9). As the separation distance between the particle and the wall becomes small, balancing the terms in Eq. (9) as $\delta \to 0$ suggests that the pressure scales as $p \propto \mu V/k$, and so the characteristic gap length-scale takes on the form

$$\ell_{n\,(\delta\to 0)} \propto R\,(k/R)^{\frac{1}{3n-2}}. \tag{18}$$

In the case of an axisymmetric object, the force on the particle scales as $f_{3D} \approx p \cdot \ell_n^2$, while for an elongated, two-dimensional shape, the force per unit length will scale as $f_{2D} \approx p \cdot \ell_n$, so that, using (18), we may write

$$f_{3D} \propto R\,(R/k)^{\frac{3n-4}{3n-2}}, \quad f_{2D} \propto (R/k)^{\frac{3n-3}{3n-2}}. \tag{19}$$

Thus we have, for the sphere or cylinder ($n = 2$), the following scalings for the forces at contact

$$f_{sphere} \propto \mu V R^{\frac{3}{2}} k^{-\frac{1}{2}}, \quad f_{cylinder} \propto \mu V R^{\frac{3}{4}} k^{-\frac{3}{4}}. \tag{20}$$

For a spherical particle, the $k^{-1/2}$ dependence agrees with the results of Goren[6] and Nir,[7] while for the cylinder we recover the result found by Sherwood.[22] The cylinder is shown to be more sensitive to the wall permeability, which may be explained due to a larger surface area exposed to the squeezed fluid-filled gap. Finally, for the flat disc, $n \to \infty$ in Eq. (19), we find that the force scales as $f \propto \mu V R^2/k$, consistent with Sherwood[8] (with a different definition of the permeability).

We note that, in performing the scaling analysis for the cylinder, neglect of end effects is justified provided ℓ_n is much smaller than the length of the cylinder. Stokes' paradox does not apply to an infinite cylinder next to a porous wall, since the force exerted by the wall is equal and opposite to that exerted by the cylinder, giving a dipolar far-field.

B. Asymptotic forms for a spherical particle

We now proceed to perform a perturbation analysis, involving the permeability parameter β for the case of a spherical particle, $n = 2$. First, an asymptotic solution for $\beta \ll 1$ (corresponding to small permeabilities, since $\beta \propto k/\delta^2$) is sought in (14) using a regular perturbation expansion,

i.e., $P = P_0 + \beta P_1 + \ldots$, resulting in the following set of perturbation problems:

$$\frac{1}{s}\frac{d}{ds}\left(s(1+s^2)^3\frac{dP_N}{ds}\right) = \begin{cases} -1 & (N=0) \\ P_{N-1} & (N \geq 1) \end{cases}, \tag{21}$$

where P_0 is the solution for a rigid, impermeable surface (in which case, $p_0 = 0$ and $V_0 = 0$). Note that for the sphere, $\ell_2 = \sqrt{2R\delta}$, $p = (24\mu V R/\delta^2)P$ and $\beta = 24kR/\delta^2$. The leading-order terms in this expansion may be found, for example by using *Mathematica*, as

$$P(s) = \frac{1}{8(1+s^2)^2} - \frac{\beta}{96(1+s^2)^3} + \frac{(3+4(1+s^2))\beta^2}{9216(1+s^2)^4} + O(\beta^3). \tag{22}$$

Next, we treat (14) for the case where $\beta \gg 1$, which corresponds to the asymptotic approach to contact ($\delta \to 0$ for fixed k). This limit leads to a seemingly singular perturbation problem with the trivial "outer" solution $P = 0$ that satisfies the far-field boundary condition outside the gap. In order to resolve the "inner" region, we re-scale (14). Re-defining the pressure as $P = \beta^{-1}P^*$ and balancing all terms in the equation, we identify the inner coordinate $\eta = \beta^{-1/4}s$, and the re-scaled equation becomes

$$\frac{1}{\eta}\frac{d}{d\eta}\left(\eta(\beta^{-1/2}+\eta^2)^3\frac{dP^*}{d\eta}\right) - P^* + 1 = 0. \tag{23}$$

We now seek a regular expansion for $\beta \gg 1$, in the form

$$P^*(\eta) = P_0^* + \beta^{-1/2}P_1^* + \beta^{-1}P_2^* + \ldots . \tag{24}$$

The perturbation equations are given, at $O(\beta^N)$, by

$$\frac{1}{\eta}\frac{d}{d\eta}\left(\eta^7\frac{dP_N^*}{d\eta}\right) - P_N^* = -\frac{1}{\eta}\frac{d}{d\eta}\left(3\eta^5\frac{dP_{N-1}^*}{d\eta} + 3\eta^3\frac{dP_{N-2}^*}{d\eta} + \eta\frac{dP_{N-3}^*}{d\eta}\right), \tag{25}$$

for $N \geq 3$, where at lower order ($N = 0, 1, 2$) the terms on the right-hand side drop out sequentially. The pressure field to $O(\beta^{-1})$ is found to be (using *Mathematica*)

$$P^*(\eta) = 1 - \left(\frac{1+2\eta^2}{2\eta^2} + \frac{3}{16\eta^6}\frac{1}{\beta^{1/2}} + \frac{9-58\eta^2+4\eta^4}{256\eta^{10}}\frac{1}{\beta}\right)e^{-\frac{1}{2\eta^2}}. \tag{26}$$

The leading term of this expansion is the "contact" approximation, which shows that the pressure becomes practically uniform within the gap, with a value $P \simeq 1/\beta$.

C. Asymptotic form for a symmetric shape near contact

The ideas illustrated above also allow us to draw conclusions about the detailed pressure distribution for symmetric shapes in the limit of $\beta \gg 1$. Beginning with Eq. (23) generalized for shapes $H = 1 + \eta^n$, and by inspection of (26), we may use $\xi = 2/(2-3n)\eta^{(2-3n)/2}$, to transform Eq. (23) into

$$\frac{d}{d\xi}\left(\xi^{(3n+2)/(2-3n)}\frac{dP_0^*}{d\xi}\right) - \xi^{(3n+2)/(2-3n)}(P_0^* - 1) = 0, \tag{27}$$

so that for general n the expression for the "contact" pressure distribution may be written as

$$P_0^* - 1 \approx \xi^{3n/(3n-2)}K_{3n/(3n-2)}(\xi), \tag{28}$$

in which $K(\xi)$ is the modified Bessel function. With the general n scaling, the expansion of P^* for $\beta \gg 1$ now has powers of $\beta^{-n/(3n-2)}$, which again reveals the force scaling at contact, since $F \approx P_0^* \cdot \eta^2 \approx \beta^{(3n-4)/(3n-2)}$, consistent with (19).

IV. EFFECT OF PARTICLE SHAPE ON THE LUBRICATION FORCE

In the case of a spherical particle ($n = 2$), the force may be calculated using Eq. (17),

$$F_2 \equiv \frac{f}{6\pi\mu V R^2/\delta} = 16\int_0^\infty s\,P(s)\,\mathrm{d}s, \tag{29}$$

where it is recalled that the reference force is the well-known lubrication result for a sphere translating perpendicular to an impermeable boundary. Performing the integration using the first few terms in the pressure field found for $\beta \ll 1$, we obtain

$$F_2 = 1 - \frac{\beta}{24} + \frac{\beta^2}{384} + O(\beta^3), \tag{30}$$

which shows that the magnitude of this force is reduced to a degree determined by the wall permeability. It is useful to re-cast this expansion as a correction factor for the Stokes drag,

$$\frac{f}{6\pi\mu RV} = \frac{R}{\delta} - \frac{R^2}{\delta^3}k + \frac{R^3}{16\delta^5}k^2 + O(k^3). \tag{31}$$

Next, for $\beta \gg 1$, under the inner scaling, the force is given by

$$F_2 = \frac{4}{\beta^{1/2}} - \frac{6}{\beta} + \frac{3}{2\beta^{3/2}} + O(\beta^{-2}), \tag{32}$$

which we re-cast as

$$\frac{f}{\sqrt{24}\pi\mu V R^{3/2}/k^{1/2}} = 1 - \frac{4\delta}{\sqrt{3/2}(kR)^{1/2}} + \frac{\delta^2}{64kR} + O(\delta^3), \tag{33}$$

where the reference force is now the drag force on a sphere at "contact." The leading term of this expansion, if cast as a correction to the Stokes drag, is $(2R/3k)^{1/2}$ and recovers the contact force derived by Goren[6] using an exact calculation, and by our scaling analysis presented in Sec. III A. The leading-order term in the asymptotic expansion for the force at "contact" may also be calculated for other shapes. For example, for the cases $n = 4$, and $n = 10$, we have, respectively, $F_4 = 0.252\beta^{-4/5}$ and $F_{10} = 0.337\beta^{-13/14}$, which confirms the generalized scaling shown in (19).

The pressure field and resulting force were computed numerically using *Mathematica* and are plotted in Figures 2 and 3, for different values of n. For the sphere ($n = 2$), the asymptotic expansions for small and large β are compared with the numerical calculations of the force, showing excellent agreement (see Fig. 3 inset). In order to cover the entire range of β values, it is necessary to include the first 6 terms in each expansion. In all cases, the pressure field (Fig. 2) follows a similar trend of flattening within the inner region ($r < \ell_n$), corresponding to the particle leading-edge becoming

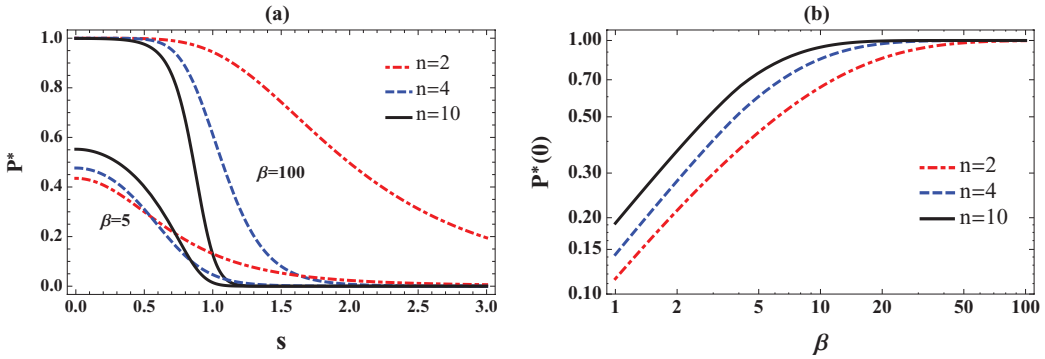

FIG. 2. The effect of shape (n), and the parameter $\beta = 12k\ell_n^2/\delta^3$, in which k is the permeability and δ is the separation distance, on the pressure within the gap between the particle and the surface. (a) The pressure distribution, $P^* = \beta P$, calculated using Eq. (14), for two representative values of β. (b) The pressure at the leading edge of the particle as a function of β, which illustrates the effect of shape on the approach to the asymptote $P \sim \beta^{-1}$.

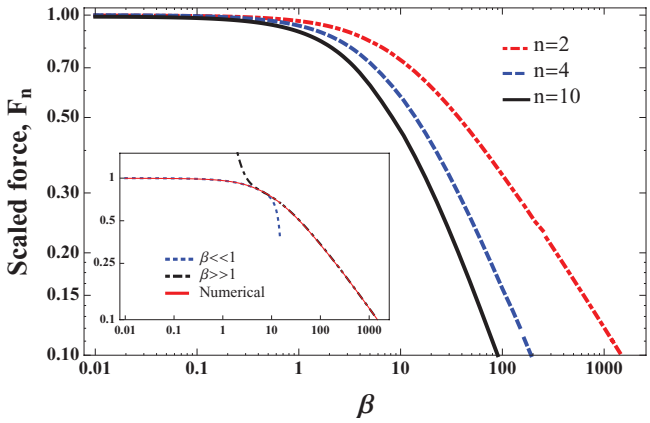

FIG. 3. The force on the particle as a function of $\beta = 12k\ell_n^2/\delta^3$, calculated using Eq. (17), for different particle shapes. Shown in the inset are the asymptotic solutions for the sphere, $n = 2$, given by Eqs. (30) and (32) in the case of small and large β, respectively, and compared to the numerical solution of Eq. (14).

flatter; an abrupt decay is then observed at a distance $r \approx \ell_n$ from the point of closest approach. The force on the particle follows from this distribution, and becomes more sensitive to the permeability parameter β as the particle becomes flatter, in agreement with the asymptotic forms.

V. PARTICLE MOTION AT CLOSE APPROACH

In general, the creeping motion of the particle at close approach (i.e., as $\delta/R \to 0$, consistent with the lubrication approximation), can be written as the force balance

$$2\pi \int_0^\infty r\,\hat{p}(r)\,\mathrm{d}r + f_{ext} = 0, \tag{34}$$

where f_{ext} is the net external force acting in the z direction on the particle, e.g., gravity or surface interactions (electrostatic, van der Waals forces, etc.). In terms of the scaled variables, as described above, the lubrication force balance can be written as

$$24c_n\pi\mu\ell_n^4\left(V_p - V_0\right)F_n/\delta^3 + f_{ext} = 0, \tag{35}$$

where we recall that $V_p = -d\delta/dt$ is the velocity of the particle and, from (17), $F_n(\beta) = c_n^{-1}\int_0^\infty s\,P(s)\,\mathrm{d}s$ accounts for the surface permeability and the particle shape, in which $\beta = 12k\ell_n^2/\delta^3$. The choice of the scaling is such that $F_n = 1$ for an impermeable surface ($\beta = 0$).

A. Sedimentation under gravity through a quiescent fluid

As a first illustration, we consider the gravitational sedimentation of a particle perpendicular to a rigid, permeable surface when there is no background permeation ($V_0 = 0$). In this case, the hydrodynamic force is directed upwards (positive), resisting the motion and proportional to $V_p = -d\delta/dt$, and $f_{ext} = -mg$, which is the buoyancy-corrected weight of the particle, and is directed downward. For general n, we write

$$\frac{d\delta}{dt} = -\frac{mg}{24c_n\pi n^{4/n}\mu R^{\frac{4(n-1)}{n}}}\frac{\delta^{\frac{4-3n}{n}}}{F_n(\beta)}. \tag{36}$$

For the case of a sphere, $n = 2$, we have $\ell_2 = (2R\delta)^{1/2}$ and $\beta = 24kR/\delta^2$. Substituting these into (36) with the leading-order term of the asymptotic solution (32) for $\beta \gg 1$, $F_2(\beta) \approx 4\beta^{-1/2}$, we find that

$$V_p = \tau_g^{-1}\,(kR)^{1/2}\,, \tag{37}$$

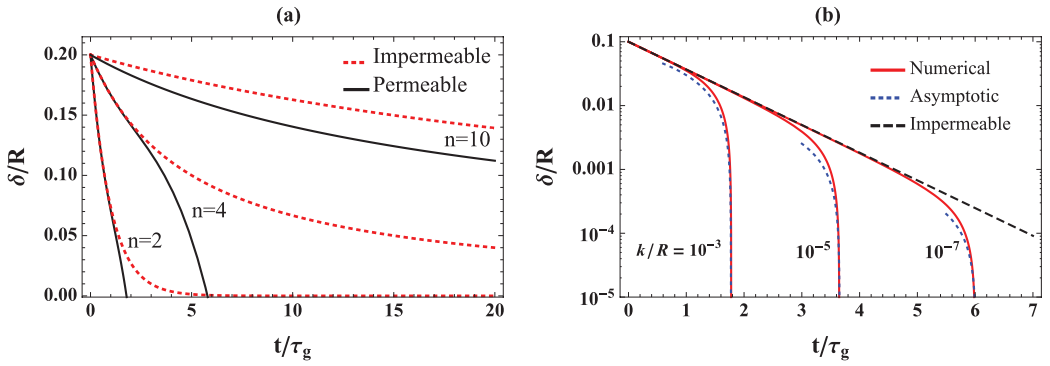

FIG. 4. The motion of the particle toward a surface due to a constant gravitational force, calculated using Eq. (36), shown in terms of a scaled separation distance, δ/R. (a) The effect of shape (n), calculated for $k/R = 10^{-5}$, as well as for an impermeable wall. (b) The case of a sphere ($n = 2$), numerical calculations and the asymptotic approach to a constant velocity, $V_p \propto (kR)^{1/2}$, for different scaled membrane permeabilities, k/R.

where $\tau_g = \sqrt{24}\pi\mu R^2/mg$ is a sedimentation time-scale. It is therefore predicted that, at close approach to the permeable surface, the sphere attains a constant velocity, which scales as $k^{1/2}$. For a non-spherical, axisymmetric object, the velocity at close approach is also constant and will vary as, for example, $V_p \propto k^{4/5}$ for $n = 4$, dictated by the force scaling at close approach; in the limit $n \to \infty$ the particle velocity is proportional to k. Similarly, the force scaling may be used to infer that the finite velocity of a cylinder will scale as $k^{3/4}$. The approach velocity is therefore predicted to be largest for the sphere. This result is intuitive, since a flatter object experiences a greater degree of interaction with the boundary, which results in a larger lubrication force. These results also suggest that a finite time would be required for contact to be made, in sharp contrast to the infinite time predicted for contact with an impermeable surface.

Given some initial position, $\delta(0)$, the sedimentation time and particle position may be calculated numerically from Eq. (36), where $F_n(\beta)$ is calculated using either the asymptotic expansions (30) and (32) (for a sphere) or numerically. Characteristic position curves for particles (with $n = 2$, 4, 10) sedimenting toward a permeable surface are shown in Fig. 4(a) and are compared with the expected trajectory for an identical particle approaching an impermeable wall ($\beta = 0$). The asymptotic result for the close approach of a sphere is computed for varying permeability by matching an initial position with the numerical solution, beyond which they are both in very good agreement (Fig. 4(b)).

B. "Permeation drag" balanced by repulsive surface forces

Next, we consider a neutrally buoyant particle carried toward the surface by the fluid permeating through the surface (at a rate V_0) under the imposed pressure, p_0. Far from the surface, the particle is force free and is simply advected by the surrounding fluid. In that case, $V \equiv V_0 - V_p = 0$ and there is no hydrodynamic force on the sphere. However, including surface interactions, e.g., electric double-layer repulsion, results in an additional force at close approach. Electrostatic repulsion may slow down the motion of the particle, so that now $V \neq 0$ and the particle begins to experience a hydrodynamic 'drag' exerted by the fluid flowing past it. This force is directed toward the surface, so that the question of whether the particle will deposit onto the surface becomes one of whether it is possible to balance the electrostatic repulsion force and the hydrodynamic permeation drag. Other surface forces, e.g., van der Waals, solvation, etc. are not included to keep the discussion simple. However, these forces may be readily incorporated into the force balance.

In the case of a spherical particle, a symmetric electrolyte and weakly charged surfaces, the electrostatic repulsion force may be approximated as[23]

$$F_{edl} \approx \frac{R\zeta}{\lambda}\exp(-\delta/\lambda), \tag{38}$$

in which

$$\zeta = 64\pi\epsilon_0\epsilon(k_bT/e)^2 \tanh\left(\frac{ze\psi_p}{4k_bT}\right)\tanh\left(\frac{ze\psi_m}{4k_bT}\right) \tag{39}$$

is a parameter characterizing the electrostatic interaction (with dimensions of energy per unit length, or force) and

$$\lambda = \left(\frac{\epsilon_0\epsilon k_bT}{2zc_0e^2}\right)^{1/2} \tag{40}$$

is the Debye length, characterizing the length-scale over which the electric double layer prevails (typically, this length is of the order of 10 nm). Here, k_b is Boltzmann's constant, T is the absolute temperature, ψ is the surface electric potential (subscripts p and m for particle and membrane, respectively), c_0 and z denotes the background electrolyte concentration and valency, respectively, e the elementary charge, ϵ_0 is the permittivity of vacuum and ϵ is the relative permittivity of the liquid.

In this case, the lubrication interaction results in a 'suction' force, directed downward, while the electrostatic repulsion is directed upward, resisting the approach of the advected particle. Using Eqs. (35) and (38), the motion of a spherical particle at close approach may be written as

$$\frac{d\hat{\delta}}{d\tau_e} = \frac{\exp(-\hat{\delta}/\hat{\lambda})}{\hat{V}_0 F_d(\hat{\delta})} - 1, \tag{41}$$

where the scaled separation distance is $\hat{\delta} \equiv \beta^{-1/2} = \delta/(24kR)^{1/2}$, which characterizes the length scale over which the lubrication force decays away from the surface, and we define a drag correction factor, $4F_d(\hat{\delta}) = F_2(\hat{\delta}^{-2})$. The same length-scale is also used to define a scaled Debye length, $\hat{\lambda} = \lambda/(24kR)^{1/2}$, signifying the ratio of characteristic decay lengths for the electrostatic and viscous forces. Finally, we have defined a scaled time, $\tau_e = V_0t/(24kR)^{1/2}$, and the parameter

$$\hat{V}_0 = \frac{\sqrt{24}\pi\mu V_0 (R/k)^{1/2}\lambda}{\zeta}, \tag{42}$$

which represents the ratio of the viscous to electrostatic forces at contact, and is directly proportional to the permeation velocity, and inversely proportional to $k^{1/2}$, illustrating that as the membrane becomes less permeable, viscous suction forces increase.

Equation (41) may be used to calculate the particle trajectory and to find the equilibrium point, if it exists, where a particle is held stationary at some distance away from the surface, by a balance of the hydrodynamic and electrostatic forces (see Fig. 5). The occurrence of such equilibria has been reported experimentally in the membrane filtration literature.[18] In such cases, the observed apparent deposition was completely reversible, and deposited particles were released simply by shutting off the permeation. In the present analysis, deposition implies that $\hat{\delta} = 0$, since a smooth surface is

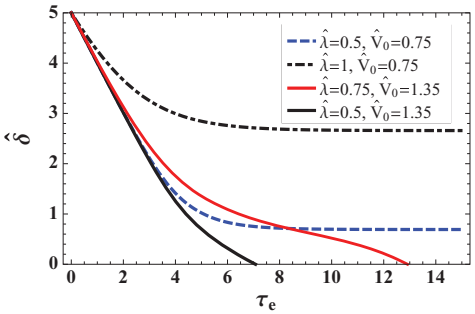

FIG. 5. The position, $\hat{\delta} = \delta/(24kR)^{1/2}$, of a sphere approaching a charged, permeable surface, carried by the permeation of the surrounding fluid, as a function of time, scaled by $V_0^{-1}(24kR)^{1/2}$. Calculations made using Eq. (41) for various values of the parameters $\hat{\lambda}$, the scaled electric-double-layer thickness, and $\hat{V}_0$, representing the ratio of viscous lubrication forces and electrostatic repulsion.

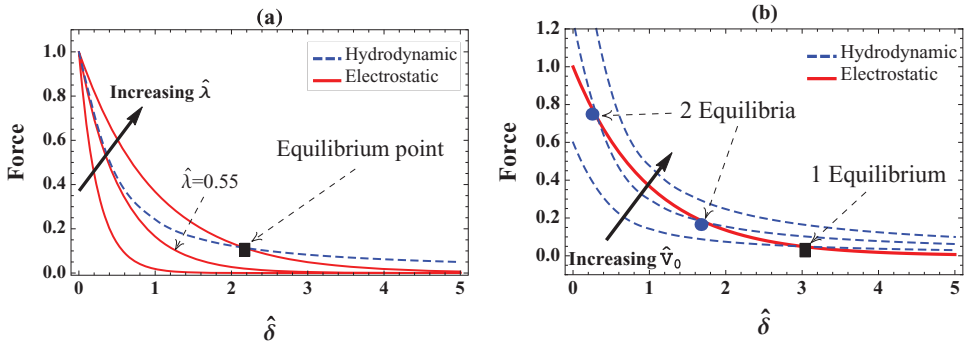

FIG. 6. The electrostatic and hydrodynamic forces as a function of separation from the surface. (a) Varying $\hat{\lambda}$, the ratio of the electrostatic and viscous decay lengths, for the case where the two forces at contact are equal, $\hat{V}_0 = 1$, illustrating the transition between regions of no equilibrium to that of a single equilibrium (signified by the intersection of the curves), as $\hat{\lambda}$ is increased. Note the curve for the electrostatic force, calculated for $\hat{\lambda} \approx 0.55$, which separates the two regions. (b) Same as in (a), with $\hat{\lambda} = 1$, illustrating the transition between a single equilibrium, two equilibria, and no equilibrium, as $\hat{V}_0$ is increased.

considered. However, for a rough surface this effective distance may correspond to the roughness scale.

Representative trajectories of a spherical particle toward a charged permeable surface have been calculated and are shown in Fig. 5. The scaled parameters $\hat{V}_0$ and $\hat{\lambda}$ are seen to influence the nature of the particle approach and whether contact would be made. For example, in cases where an equilibrium position is reached away from the surface, its distance from the surface increases in the presence of a thicker electric double layer (larger $\hat{\lambda}$). In cases where deposition occurs (signified by a particle reaching $\hat{\delta} = 0$), the trajectory exhibits two distinctive forms. The first, occurring for larger $\hat{\lambda}$, follows a smooth deceleration of the particle until contact is made, whereas at smaller $\hat{\lambda}$ an initial deceleration phase is followed by acceleration to contact. The latter behavior may be explained by considering the equilibrium properties of the system. The range of the electrostatic interaction is represented here by the parameter $\hat{\lambda}$, the ratio of the Debye length to $(kR)^{1/2}$, a length scale representative of the distance from the boundary over which permeation-induced suction is dominant. An illustration of the interplay between the hydrodynamic and electrostatic forces is given in Fig. 6, which shows their decay away from the surface and the effect of varying the range of electrostatic repulsion (increasing $\hat{\lambda}$) and the magnitude of viscous suction (increasing $\hat{V}_0$). Comparing the decay of the forces provides visual indication of whether an equilibrium exists, since it occurs when there is an intersection of the force curves. We note that the viscous suction force is scaled such that it has a value of 1 at contact and an initial slope of $-3/2$ (given by the re-scaled close approach asymptotics, (33)), whereas the electrostatic repulsion has a value of $1/\hat{V}_0$ at contact and decays with an initial slope of $-1/\hat{\lambda}$. Thus, for $\hat{V}_0 \approx 1$ and $\hat{\delta} \ll 1$, it follows from Eq. (41) with the particle velocity set to zero and the leading order term of (33), that

$$\hat{\delta}_{eq} \approx \frac{1 - \hat{V}_0}{\hat{\lambda}^{-1} - \frac{3}{2}\hat{V}_0}, \tag{43}$$

which may be used to find the approximate equilibrium point where the force curves intersect. The equilibrium point may occur for $\hat{V}_0$ just over or just under 1, depending respectively on whether $\hat{\lambda}$ is greater than or less than 2/3. The same applies for the stability of the equilibrium, with solutions for $\hat{V}_0 > 1$ being unstable. Due to the ultimate shape of the force curves (see Fig. 6), there are other solutions occurring at larger values of $\hat{\delta}$. As illustrated in Fig. 6(a), given identical electrostatic and hydrodynamic forces at contact ($\hat{V}_0 = 1$), with increasing $\hat{\lambda}$ the curves proceed from having no intersection to having a single intersection, with the transition occurring at $\hat{\lambda} \approx 0.55$. In a similar fashion, Fig. 6(b) shows that, given a characteristic EDL thickness (here, $\hat{\lambda} = 1$), increasing the relative magnitude of the lubrication force ($\hat{V}_0$) shifts the curves from having a single intersection

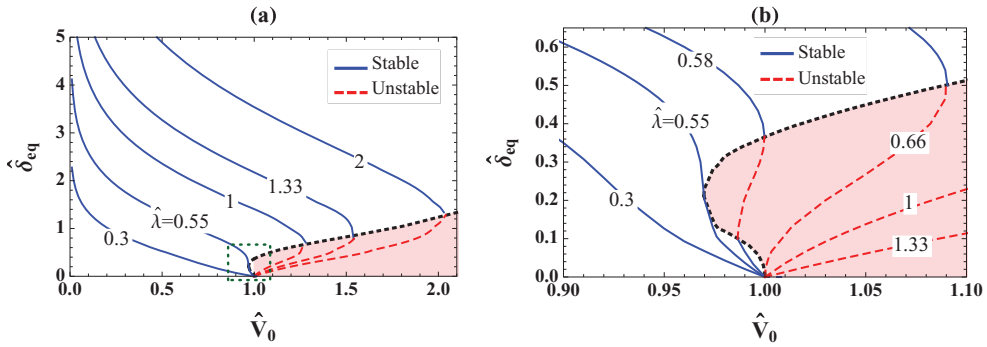

FIG. 7. The equilibrium separation distance, $\hat{\delta}_{eq}$, of a sphere near a charged, permeable surface, in the presence of a background permeation of the surrounding fluid. (a) Calculations made using a steady-state Eq. (41) for various values of $\hat{\lambda}$, the scaled electric-double-layer thickness, and $\hat{V}_0$, representing the viscous lubrication forces and electrostatic repulsion. (b) Same as (a), magnification of the region near $\hat{V}_0 = 1$ (dashed rectangle in (a)), showing the possibility of three equilibria. The calculations show regions of stable and unstable (shaded, red online) equilibria. The value $\hat{\lambda} \approx 0.55$ signifies the transition from a region of a single, stable equilibrium to a region of three equilibria, followed by a transition to two equilibria at $\hat{\lambda} = 2/3$.

(one stable equilibrium) to having two intersections (two equilibria, stable and unstable) until, finally, the curves do not intersect and no equilibrium exists.

Furthermore, the range of the electrostatic and hydrodynamic interactions creates a transition between a regime where a single, stable equilibrium exists as long as $\hat{V}_0 < 1$, and a regime where two equilibria are possible, one stable and one unstable (see Fig. 7(a)). However, looking closely at the region around $\hat{V}_0 = 1$ reveals that this transition occurs through an intermediate region, in which three equilibria exist, two stable and one unstable (see Fig. 7(a)). This region is bounded on one side by the value for which the force curves first intersect (at $\hat{\lambda} \approx 0.55$ where the three solutions reduce to one through a saddle-node bifurcation), and on the other side by $\hat{\lambda} = 2/3$ where their slope toward contact converges. When $\hat{\lambda} < 0.55$, the trajectory leading to deposition will follow a monotonic deceleration; however, for $\hat{\lambda} > 2/3$, deposition may follow a two-stage deceleration/acceleration that appears to emerge from the bifurcation of the initially stable branch which, upon increase of $\hat{V}_0$ beyond a critical value, enters the unstable region (shaded red in Fig. 7). For a fixed value of $\hat{V}_0 > 1$, deposition will occur when the initial position is smaller than the unstable equilibrium point. For an initial particle position larger than the value of the smaller, unstable equilibrium point, the trajectory will tend to the stable equilibrium point.

VI. CONCLUDING REMARKS

The present work explores the hydrodynamic interaction of a rigid particle and a thin, permeable membrane. A symmetric particle shape is prescribed and its effect on the hydrodynamic interaction is explored using the lubrication approximation. Specifically, the force on the particle and its motion toward contact are elucidated. An approximate solution is found for the case of a sphere, in the limits of small permeability and near contact. In all cases, the surface permeability lowers the lubrication force on the particle, compared to an impermeable boundary. For the generalized shape, the hydrodynamic force at near contact scales as $(R/k)^{(3n-4)/(3n-2)}$, becoming more sensitive to the wall permeability as the particle becomes flatter (increasing n). We find that for a sedimenting particle, a finite velocity is attained, regardless of shape, which is shown to scale as $k^{1/2}$ for a sphere, $k^{3/4}$ for a cylinder and as k for a flat disc. These results indicate that a finite time exists for the particle to make contact with the permeable surface.

Finally, the advection of a particle toward a charged, permeable surface is considered, and the possible equilibrium position of a particle is demonstrated, resulting from a balance of a repulsive surface force and the drag exerted by the fluid permeating through the membrane. It is shown that when a long-range electrostatic interaction is present (as may be found in dilute electrolyte solutions) two equilibrium positions may exist; a stable equilibrium will prevail up to some critical ratio of

the hydrodynamic and electrostatic forces, whence it will transition to an unstable region leading to deposition. It is further found that there exists a critical scaled electrostatic screening length, $\hat{\lambda} \approx 0.55$, below which equilibrium is always stable when the ratio of the viscous to electrostatic forces at contact, $\hat{V}_0 < 1$. Conversely, when $\hat{\lambda} > 2/3$, deposition may occur when $\hat{V}_0$ exceeds some critical value. An intermediate region is found for $0.55 < \hat{\lambda} < 2/3$, where three equilibria are possible, two unstable and one stable. Initial particle positions within regions of unstable equilibria are found to lead to deposition in all cases. These results are useful for estimating the hydrodynamic contribution to deposition propensity of colloidal particles in membrane filtration processes.

ACKNOWLEDGMENTS

The research leading to these results has received funding from the European Union Seventh Framework Programme (FP7/2007-2013) under Grant No. 275911. H.E.H. gratefully acknowledges support from Howard Stone's research grants and Princeton University to cover his enjoyable and productive visit there during the Fall semester of 2011. J.R.L. also gratefully acknowledges support from Princeton University to cover a sabbatical visit during the Spring semester 2013. H.A.S. thanks the NSF via Grant No. CBET-1234500. We thank John Sherwood and the anonymous referees for helpful feedback on this work. We also thank an anonymous reviewer for his assistance with Eq. (27) of this paper.

[1] H. Brenner, "The slow motion of a sphere through a viscous fluid towards a plane surface," Chem. Eng. Sci. **16**, 242–251 (1961).
[2] N. Lecoq, R. Anthore, B. Cichocki, P. Szymczak, and F. Feuillebois, "Drag force on a sphere moving towards a corrugated wall," J. Fluid Mech. **513**, 247–264 (2004).
[3] J. Urzay, S. G. Llewellyn Smith, and B. J. Glover, "The elastohydrodynamic force on a sphere near a soft wall," Phys. Fluids **19**, 103106 (2007).
[4] C. J. Cawthorn and N. J. Balmforth, "Contact in a viscous fluid. Part 1. A falling wedge," J. Fluid Mech. **646**, 327–338 (2010).
[5] N. J. Balmforth, C. J. Cawthorn, and R. V. Craster, "Contact in a viscous fluid. Part 2. A compressible fluid and an elastic solid," J. Fluid Mech. **646**, 339–361 (2010).
[6] S. L. Goren, "The hydrodynamic force resisting the approach of a sphere to a plane permeable wall," J. Colloid Interface Sci. **69**, 78–85 (1979).
[7] A. Nir, "On the departure of a sphere from contact with a permeable membrane," J. Eng. Math. **15**, 65–75 (1981).
[8] J. D. Sherwood, "The force on a sphere pulled away from a permeable half-space," PhysicoChem. Hydrodyn. **10**, 3–12 (1988).
[9] A. C. Michalopoulou, V. N. Burganos, and A. C. Payatakes, "Creeping axisymmetric flow around a solid particle near a permeable obstacle," AICHE J. **38**, 1213–1228 (1992).
[10] A. C. Michalopoulou, V. N. Burganos, and A. C. Payatakes, "Hydrodynamic interactions of two permeable particles moving slowly along their centerline," Chem. Eng. Sci. **48**, 2889–2900 (1993).
[11] A. M. J. Davis, "Axisymmetric flow due to a porous sphere sedimenting towards a solid sphere or a solid wall: Application to scavenging of small particles," Phys. Fluids **13**, 3126–3133 (2001).
[12] L. Elasmi and F. Feuillebois, "Green function for the Stokes flow near a porous slab," Z. Angew. Math. Mech. **81**, 743–752 (2001).
[13] L. Elasmi and F. Feuillebois, "Integral equation method for creeping flow around a solid body near a porous slab," Q. J. Mech. Appl. Math. **56**, 163–185 (2003).
[14] A. Debbech, L. Elasmi, and F. Feuillebois, "The method of fundamental solution for the creeping flow around a sphere close to a membrane," Z. Angew. Math. Mech. **90**, 920–928 (2010).
[15] Z. Y. Yan, S. Weinbaum, P. Ganatos, and R. Pfeffer, "The three-dimensional hydrodynamic interaction of a finite sphere with a circular orifice at low Reynolds number," J. Fluid Mech. **174**, 39–68 (1987).
[16] G. Z. Ramon and E. M. V. Hoek, "On the enhanced drag force induced by permeation through a filtration membrane," J. Membr. Sci. **392-393**, 1–8 (2012).
[17] M. Shannon, P. W. Bohn, M. Elimelech, J. G. Georgiadis, B. J. Marinas, and A. M. Mayes, "Science and technology for water purification in the coming decades," Nature (London) **452**, 301–310 (2008).
[18] S. Wang, G. Guillen, and E. M. V. Hoek, "Direct observation of microbial adhesion to membranes," Environ. Sci. Technol. **39**, 6461–6469 (2005).
[19] H. A. Stone, "On lubrication flows in geometries with zero local curvature," Chem. Eng. Sci. **60**, 4838–4845 (2005).
[20] L. Leal, *Advanced Transport Phenomena: Fluid Mechanics and Convective Transport Processes* (Cambridge University Press, New York, 2007).
[21] A. Oron, S. H. Davis, and S. Bankhoff, "Long-scale evolution of thin liquid films," Rev. Mod. Phys. **69**, 931–980 (1997).
[22] J. D. Sherwood, "The hydrodynamic forces on a cylinder touching a permeable wellbore," Phys. Fluids A **2**, 1754–1759 (1990).
[23] J. Israelachvili, *Intermolecular and Surface Forces*, 3rd ed. (Academic Press, 2011).